European Journal of Pharmaceutics and Biopharmaceutics

Dopamine-loaded lipid based nanocarriers for nose-to-brain delivery of the neurotransmitter: a comparative study

--Manuscript Draft--

Manuscript Number:	
Article Type:	Research Paper
Keywords:	Liposomes; Solid lipid nanoparticles; Dopamine; X-Ray Photoelectron Spectroscopy Analysis; Cytotoxicity; Olfactory cells; Uptake
Corresponding Author:	Adriana Trapani University of Bari Bari, Italy
First Author:	Adriana Trapani
Order of Authors:	Adriana Trapani
	Elvira De Giglio
	Stefania Cometa
	Maria Addolorata Bonifacio
	Laura Dazzi
	Sante Di Gioia
	Md Niamat Hossain, Hossain
	Rosalia Pellitteri
	Sophia Antimisiaris
	Massimo Conese
Abstract:	Both dopamine (DA) loaded Solid Lipid Nanoparticles (SLN) and liposomes (Lip), intended to enhance the nose-to-brain delivery of neurotransmitter for Parkinson disease patients, were already characterized in vitro in some extent by us. Herein, to gain insight into the structure of SLN, X-ray Photoelectron Spectroscopy Analysis was carried out and DA-SLN (SLN 1) were found to exhibit high amounts of the neurotransmitter on the surface, whereas the external side of Glycol Chitosan (GCS) containing SLN (SLN 2) possessed only few amounts. However, SLN 2 were characterized by the highest encapsulation DA efficiency (i.e., 81%). Furthermore, in view of intranasal administration, mucoadhesion tests in vitro were also conducted for SLN and Lip formulations, evidencing high muchoadesive effect exerted by SLN 2. Concerning ex-vivo studies, SLN and Lip were found to be safe for Olfactory Ensheathing Cells and fluorescent SLN 2 were taken up in a dose-dependent manner reaching the 100% of positive cells, while Lip 2 were internalised by 70% OECs with six-times more lipid concentration. Hence, SLN 2 formulation containing DA and GCS may constitute interesting formulations for further studies and promising dosage form for non-invasive nose-to-brain neurotransmitter delivery.
Suggested Reviewers:	Carmen Gutierrez Millan carmen.gutierrez@usal.es
	Alvaro Mata a.mata@qmul.ac.uk
	Maria Teresa Moreno Flores mteresa.moreno@uam.es
	Udo Bakowsky ubakowsky@aol.com
	Marcos Garcia Fuentes marcos.garcia@usc.es

Opposed Reviewers:	

DIPARTIMENTO DI
FARMACIA-SCIENZE DEL FARMACO

Corresponding Authors:

Prof. Adriana Trapani

Department of Pharmacy-Drug Sciences

University of Bari "Aldo Moro", Bari, Italy

Tel.: +39-0805442114. Fax: +39-0805442724.

E-mail: adriana.trapani@uniba.it.

Prof. Sante Di Gioia

Department of Medical and Surgical Sciences

University of Foggia, 71122 Foggia, Italy

Tel.: +39-0881558019. Fax: +39-0881588074.

E-mail: sante.digioia@unifg.it

October, 26th 2020

To the Editor in Chief of

European Journal of Pharmaceutics and Biopharmaceutics

Prof. A. Goepferich,

University of Regensburg Faculty of Chemistry and Pharmacy, Universitätsstrasse 31, 93040, Regensburg, Germany

Dear Prof. Goepferich,

Enclosed please find a copy of the manuscript entitled **"Dopamine-loaded lipid based nanocarriers for nose-to-brain delivery of the neurotransmitter: a comparative study"** by A. Trapani et al. submitted for publication to *European Journal of Pharmaceutics and Biopharmaceutics*.

The paper is submitted as a research paper and it deals with the results of investigations concerning *in vitro* and *ex vivo* evaluation of dopamine (DA) loaded solid lipid nanoparticles (SLN) formulated in the presence and in the absence of the polysaccharide Glycol Chitosan (GCS) for a potential nasal administration to patients affected by Parkinson disease (PD). Moreover, for sake of comparison,

liposomes containing DA, already studied by some of the co-authors, were also subjected to the same assays employed for SLN. In particular, the *in vitro* evaluation carried out on SLN formulated in the presence of GCS (SLN 2) in Simulated Nasal Fluid allowed to evidence better mucoadhesive properties of these particles. Again, it was assessed that SLN 2 possessed a physical stability higher than the vesicle formulations investigated. Furthermore, no cytotoxicity was detected after exposure of the SLN to Olfactory Ensheathing Cells (OECs). Cytofluorimetric analysis indicated that fluorescent SLN were internalized by OECs in a dose dependent manner in a bigger amount than liposomal formulations. All these results, taken together, suggest that the PEGylated SLN 2 possess a promising potential as delivery systems of the neurotransmitter, better than the vesicle formulations following the nasal route of administration. Hence, SLN 2 constitute an interesting candidate for the treatment of a neurological disorder such as PD.

We believe that the paper has elements which fall within the scope of the. *European Journal of Pharmaceutics and Biopharmaceutics.* In our opinion, the study can be of interest for scientists involved in carrier mediated nose-to-brain delivery of pharmaceutics for the treatment of neurological disorders and especially for PD.

This manuscript (or its contents in some other form) has not been published previously by any of the authors and/or is not under consideration for publication in another journal at the time of submission. All the authors have seen and approved the submission of the manuscript to *European Journal of Pharmaceutics and Biopharmaceutics.*

We look forward to hearing from you in the next future,

Sincerely yours,

Prof. Adriana Trapani
Prof. Sante Di Gioia

Graphical Abstract

Click here to access/download;Graphical Abstract;Graphical Abstract JPEG.jpg

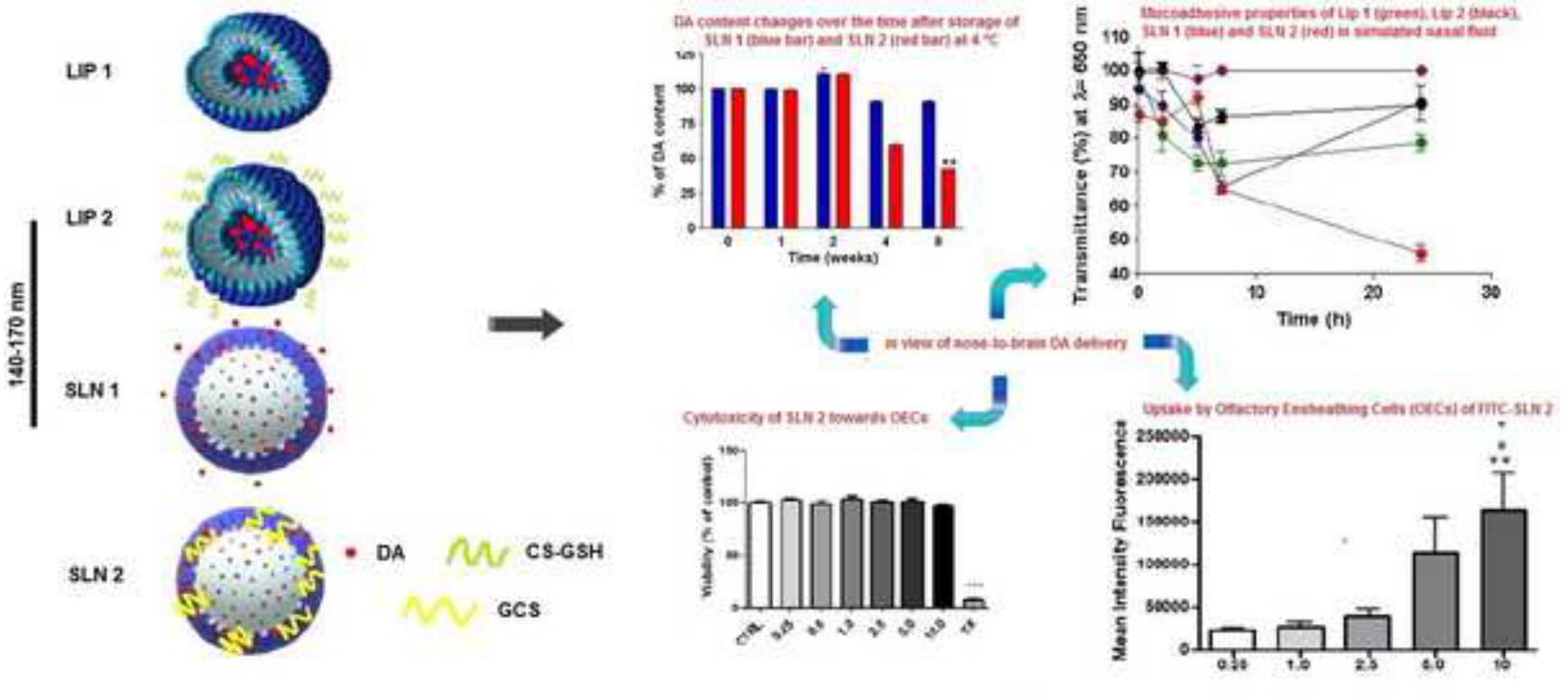

Dopamine-loaded lipid based nanocarriers for nose-to-brain delivery of the neurotransmitter: a comparative study

Adriana Trapani[a*], Elvira De Giglio[b], Stefania Cometa[c], Maria Addolorata Bonifacio[b], Laura Dazzi[d], Sante Di Gioia[e*], Md Niamat Hossain[e], Rosalia Pellitteri,[f] Sophia G. Antimisiaris,[g] Massimo Conese[e]

[a]Department of Pharmacy-Drug Sciences, University of Bari "Aldo Moro", Bari, Italy

[b]Chemistry Department, University of Bari "Aldo Moro", via Orabona, 4, 70125 Bari, Italy

[c]Jaber Innovation s.r.l., 00144 Rome, Italy

[d]Department of Life and Environmental Sciences, Section of Neuroscience and Anthropology, University of Cagliari, Monserrato (Cagliari), Italy

[e]Department of Medical and Surgical Sciences, University of Foggia, Foggia, Italy

[f] Institute for Biomedical Research and Innovation (IRIB-CNR), 95126 Catania, Italy

[g]Foundation for Research and Technology Hellas, Institute of Chemical Engineering Sciences, FORTH/ICE-HT, Rio 26504, Greece

*Corresponding authors:

*A.T.: Email: adriana.trapani@uniba.it

*S.D.G.: Email: sante.digioia@unifg.it

Abstract

Both dopamine (DA) loaded Solid Lipid Nanoparticles (SLN) and liposomes (Lip), intended to enhance the nose-to-brain delivery of neurotransmitter for Parkinson disease patients, were already characterized *in vitro* in some extent by us. Herein, to gain insight into the structure of SLN, X-ray Photoelectron Spectroscopy Analysis was carried out and DA-SLN (SLN 1) were found to exhibit high amounts of the neurotransmitter on the surface, whereas the external side of Glycol Chitosan (GCS) containing SLN (SLN 2) possessed only few amounts. However, SLN 2 were characterized by the highest encapsulation DA efficiency (*i.e.,* 81%). Furthermore, in view of intranasal administration, mucoadhesion tests *in vitro* were also conducted for SLN and Lip formulations, evidencing high muchoadesive effect exerted by SLN 2. Concerning *ex-vivo* studies, SLN and Lip were found to be safe for Olfactory Ensheathing Cells and fluorescent SLN 2 were taken up in a dose-dependent manner reaching the 100% of positive cells, while Lip 2 were internalised by 70% OECs with six-times more lipid concentration. Hence, SLN 2 formulation containing DA and GCS may constitute interesting formulations for further studies and promising dosage form for non-invasive nose-to-brain neurotransmitter delivery.

Keywords: *Liposomes, Solid lipid nanoparticles, Dopamine, X-Ray Photoelectron Spectroscopy Analysis, Cytotoxicity, Olfactory cells, Uptake.*

List of chemical compounds studied in the article: Dopamine hydrochloride (Compound CID: 65340), Chitosan (Compound CID: 129662530), Hydroxyethylcellulose (Compound CID: 4327536), Dimethyl Sulphoxide (Compound CID:679).

1. Introduction

Parkinson's disease (PD) is a progressive neurodegenerative disorder that predominantly affects older adults, particularly in economically developed Countries [1]. The PD patient shows motor symptoms such as tremor, rigidity, bradykinesia, and postural instability as well as several non-motor symptoms as gastrointestinal ones [2]. The main PD hallmarks are the loss of dopaminergic neurons in the Substantia Nigra *pars compacta* and the presence in the brain of Lewy bodies abnormal protein aggregates including alpha-synuclein and ubiquitin [3-5]. However, the pathogenesis of PD is still unknown, and the most followed therapeutic approach involves the so-called "dopamine (DA) replacement strategy" which allows to control PD motor symptoms. In particular, levodopa (L-Dopa), a biological precursor of DA, still constitutes the most effective and reference drug [3, 5]. DA, indeed, is unable to overcome the Blood-Brain-Barrier (BBB) due to its physicochemical and metabolic features [4], whereas L-Dopa can cross the BBB exploiting an active transport system and is converted in the brain to DA by L-Dopa-decarboxylase mediated decarboxylation [4, 6, 7]. It should be noted that even in pathologies as stroke, PD, Alzheimer's disease where the BBB is compromised and permeable enough, it still constitutes an obstacle to drug delivery into the brain [8]. In this regard, the promising role played by nanostructured drug delivery systems has been pointed out [9]. Thus, most interest has been focused on the development of DA-loaded nanocarriers as innovative PD treatment, since they may be able to cross the BBB enabling also a sustained delivery of the neurotransmitter to the brain [4, 10-14]. In addition, it has also been pointed out that the intranasal route of administration may constitute a useful approach for a non-invasive method of bypassing BBB and to achieve the delivery of therapeutic agents into the brain [7, 15, 16]. Using this administration route, delivery of therapeutics to the brain occurs exploiting the connections between the olfactory epithelium located on the roof of the nasal cavity and the olfactory and trigeminal nerve components [7, 15, 16].

Apart from this, a challenging aspect in DA chemical manipulations is that, in the presence of molecular oxygen, DA undergoes a spontaneous autoxidation reaction under neutral/alkaline conditions. In such autoxidation process, the key steps are the aminochrome formation and the successive synthesis of polymer compounds (e.g., neuromelanins) through reactive oxygen species (ROS) which can damage cellular components and may be crucial in the development of neurodegenerative diseases as PD [17-19]. In this regard, it has been hypothesized that DA encapsulation in nanocarriers may reduce the autoxidation reaction of the same neurotransmitter [18]. Our interest for DA brain delivery by nanocarriers [4, 11, 12] led us to evaluate the protective effect toward the autoxidation reaction of DA encapsulation in liposomes. We found that both the uncoated and, in particular, the chitosan-glutathione (CS-GSH)-coated ones showed a prolonged stability

against oxidative damage [18]. Definitively, DA-loaded nanocarriers administered by nasal route may represent an innovative and disease-modifying approach for PD treatment, because it may allow not only the BBB crossing and neurotransmitter sustained delivery but also may reduce the oxidative damage, leading to neuroinflammation. In addition, it should be considered that advances in the preparative methods of nanomaterials allowed the availability of very small in size nanocarriers with interesting features including prolonged circulation, sustained release and BBB crossing [20-22].

Among the DA-loaded nanocarriers employed to improve PD treatment, mainly polymeric nanocarriers have been investigated including PLGA-, chitosan-, glycol chitosan-, polyvinylpyrrolidone-polyacrylic acid and cellulose acetate phthalate-based nanoparticles (NPs) following parenteral or alternative administration routes [4, 11-14] or intracranial implantation [10]. However, to the best of our knowledge, the potential of lipid-based nanocarriers in nose-to-brain delivery of the neurotransmitter has not been deeply investigated. Lipid-based nanocarriers are at the forefront of the nanotechnology applied in drug delivery and especially for delivery to the brain [23]. Thus, for instance, liposomes are colloidal carriers extensively used, besides cyclodextrins [24] and polymeric micelles [25], to improve the formulation of hydrophobic drugs for their non-toxic, non-immunogenic, and biodegradable features. However, liposomes possess some drawbacks including the leakage of the encapsulated therapeutic molecule and the sensitivity of phospholipids to heat and radiation during sterilization processes. In recent years, solid lipid nanoparticles (SLN) have attracted increasing interest since they possess several advantages including enhanced safety and stability, controlled drug release, reduced leakage of the encapsulated drug and can be applied for both hydrophobic and hydrophilic drugs [26]. Moreover, SLN can be administered by several routes, including the oral one which matches the patient compliance and the approval of the pharmaceutical industry [27, 28]. In the present work, to shed light into the possible role played by lipid based nanocarriers in nose-to-brain DA delivery, we report the results of a comparative study aimed at evaluating the potential use of DA-loaded liposomes and DA-loaded SLN in nose-to-brain delivery of the neurotransmitter. Liposomes were prepared by the Dried Reconstituted Vesicles (DRV) method using a mixture of phosphatidyl choline, phosphatidyl glycerol and cholesterol as lipid components according to our previous work [18]. SLN were prepared following the melt homogenization method using Gelucire® 50/13, a self-emulsifying lipid, as lipid component taking into account that the use of such lipid matrix may be a promising approach for increasing the drug loading of hydrophilic active principles such as the neurotransmitter DA [29, 30]. Gelucire® 50/13, indeed, is composed of PEG-esters (stearoyl polyoxyl-32 glycerides), a small glyceride fraction and free PEG chains and it is able to self-emulsify with aqueous media and the resulting SLN may be considered PEGylated SLN. Besides unmodified liposomes and SLN, the chitosan-glutathione conjugate (CS-GSH)-coated

DA-loaded liposomes as well as Glycol Chitosan (GCS)-associated DA-loaded Gelucire® 50/13 SLN were also evaluated. Both CS-GSH coating and GCS association were employed as an approach to limit the immature leakage of the encapsulated neurotransmitter from liposomes and SLN, respectively. The polycation GCS was preferred to the parent polymer CS for the higher aqueous solubility in neutral and physiological conditions [29]. Moreover, in view of intranasal administration, the DA-loaded nanocarriers were subjected to mucoadhesion and X-Ray photoelectron spectroscopy (XPS) studies as well as their cytotoxicity and uptake by glial cells involved in nose-to-brain delivery, namely Olfactory Ensheathing Cells (OECs), were also determined.

2. Materials and methods

2.1. Materials

Dopamine hydrochloride, Cholesterol (Chol), Glycol chitosan, Fluorescein 5(6)-isothiocyanate (FITC), 6-Coumarin (6-COUM), carboxyl ester hydrolase (E.C. 3.1.1.1, 15 units/mg solid) from porcine liver, Tween® 85 as well as the salts used for buffer preparation were purchased from Sigma-Aldrich (Milan, Italy). Soybean phosphatidyl choline (PC, 70% of purity) and phosphatidyl glycerol (PG, 99.6% of purity) were obtained from Lipoid (Germany). Gelucire® 50/13 was a gift by Gattefossè (Milan, Italy). Hydroxyethyl cellulose (HEC, Natrosol 250) was provided by Aakon Polichimica (Milan, Italy). According to manufacturer instructions, the viscosity of a solution of HEC at the concentration of 2% in water was equal to 5500 mPa•sec. The polycarbonate filters for liposome extrusion (LiposoFast-Basic extruder) were purchased from Avestin (Germany). Chitosan-glutathione conjugate (CS-GSH) was prepared as previously reported [31].

Throughout this work, double distilled water was used. All other chemicals were of reagent grade.

2.2. Preparation of liposomes

The liposomes were prepared following the Dried Reconstituted Vesicles (DRV) method as previously reported [18, 32]. Briefly, liposomes made of a mixture of PC/PG/Chol at 9:1:10 mol:mol:mol, respectively, were prepared by mixing all the lipids [each dissolved in chloroform/methanol (2:1, v/v)] in a 50 mL round-bottom flask and evaporated (rotary evaporator set at 40°C) leading to a thin-film formation. These lipid films were hydrated by adding 10% (v/v) phosphate buffered saline (PBS, pH 6, 1 mM) at room temperature giving rise to plain Multilamellar Vesicles (MLVs) which were then reduced in size by probe sonication (at least two 10 min cycles of sonication were necessary) followed by a centrifugation step, (14000 rpm,6 min) providing so plain Small Unilamellar Vesicles (SUV). To prepare uncoated DA-loaded liposomes (Lip 1), 0.5 mL of a light protected aqueous DA solution in d-H_2O (10 mg/mL) were then mixed with 1 mL of the SUV

liposomes, and the resulting mixture was lyophilized overnight at −48 °C and 0.150 mBar pressure, and subjected to controlled re-hydration. Then, the liposomes were extruded through 400 nm and then 200 nm pore size polycarbonate filters, by LiposoFast-Basic extruder and the resulting suspensions were ultracentrifuged. The precipitated purified liposomes were the uncoated DA-loaded liposomes. To prepare the CS-GSH coated DA-loaded liposomes (Lip 2), the uncoated DA loaded vesicles were incubated with the coating solutions for 1 h under mechanical stirring at room temperature under light protection. The coating solutions of CS-GSH were separately prepared dissolving a suitable amount of the polysaccharide at pH 4.4 in order to prepare two solutions at 0.1 and 0.3 mg/mL concentration, respectively and the resulting solutions were stirred overnight at room temperature and then filtered (0.45 μm pore size). For uptake studies, fluorescent COUM-loaded Lip 1 and Lip 2 (*i.e.,* 6-COUM Lip 1 and 6-COUM Lip 2) were prepared following the same protocol above described with the following modifications. 10 mg of 6-COUM/mL of chloroform/methanol were employed instead of DA aqueous solution and they were added during thin-film formation.

2.3. Preparation of SLN

The preparation of DA-loaded Gelucire® 50/13 SLN (SLN 1) and GCS associated DA-loaded Gelucire® 50/13 SLN (SLN 2) was made following the melt homogenization method as previously reported [33]. Briefly, Gelucire® 50/13 (60 mg) was melted at 70 °C and, in a separate vial, DA (10 mg), the surfactant (Tween® 85, 60 mg) and 1.37 mL diluted acetic acid, 0.01%, w/v, were prepared and, then, heated at 70 °C. The resulting mixture was added to the melted phase at 70 °C in order to obtain an emulsion by homogenization at 12300 rpm for 2 min with an UltraTurrax model T25 apparatus (Janke and Kunkel, Germany). Next, the nanosuspension was cooled at room temperature and the resulting SLN 1 centrifuged (16,000 × g, 45 min, Eppendorf 5415D, Germany) and the obtained pellet was re-suspended in distilled water for further studies.

To prepare the GCS-DA-SLN (SLN 2), 1.37 g of a previously formed solution of GCS (5 mg/mL in AcOH 0.01, w/v) was added to the aqueous phase containing DA (10 mg), the surfactant (Tween® 85, 60 mg) and 1.37 mL of water. Afterwards, the procedure was the same as reported above for DA-SLN. Control SLN were either the ones without both DA and GCS (namely, plain SLN) or the ones without DA, but containing GCS (namely, GCS-SLN). For biological experiments, fluorescent SLN (i.e., FITC-SLN) were prepared following the same protocol of GCS-DA-SLN, but replacing 10 mg of DA in the aqueous phase with the same amount of FITC.

2.4. Physicochemical characterization of lipid carriers

The quantitative determination of DA and 6-COUM were carried out by HPLC and fluorimetric assays, respectively, as previously reported [18, 34].

Particle size and polydispersity index (PDI) of liposomes and SLN were determined by using a ZetasizerNanoZS (ZEN 3600, Malvern, UK) apparatus according to photon correlation spectroscopy (PCS) mode. The particle size of liposomes was measured at 25 °C after dilution with PBS (pH 6) to give a 0.4 mg/mL of final lipid concentration, whereas in the case of SLN the particle size and PDI was measured after dilution 1:1 (v:v) with double distilled water. The determination of the zeta-potential of liposomes was performed at 25 °C using laser Doppler anemometry (ZetasizerNanoZS, ZEN 3600, Malvern, UK) after dilution at the same concentration employed for size measurement in potassium phosphate buffer. In the case of SLN the zeta-potential was determined after dilution of the sample 1:20 (v:v) in the presence of KCl (1 mM, pH 7) [35, 36].

2.5. *Physical stability of SLN formulations*

For SLN 1 and SLN 2 the physical stability was evaluated measuring their particle size after incubation upon storage at 4° C up to 2 months as well as monitoring the neurotransmitter content in the particles over the time. The particle size was measured at different time intervals during the duration of the study according to that reported in Section 2.4.

For DA content monitoring, freshly prepared samples of SLN 1 and SLN 2 were centrifuged (16,000 × g, 45 min, Eppendorf 5415D, Germany) and the resulting pellets were re-suspended in distilled water and freeze-dried for 72 h (T = -46 °C and P = 0.1 mBar, Lio Pascal 5P, Milan, Italy). Then, the collected powders were evaluated for their stability upon storage at 4°C for two months.

To evaluate the neurotransmitter content in the particles at different time points, appropriate aliquots of DA containing SLN were incubated in the presence of 1 mL of carboxyl ester hydrolase solution (0.6 mg/mL phosphate buffer pH 5.0) [33] at 37 °C for 30 min and, afterwards, centrifuged as described in Section 2.3. The obtained supernatant was analyzed by HPLC to determine the DA contents [18].

2.6. In vitro evaluation of mucoadhesive properties of DA liposomes and SLN

The mucoadhesive properties of DA-loaded liposomes and SLN were evaluated in Simulated Nasal Fluid (SNF) by turbidimetric measurements [31], SNF was prepared dissolving $CaCl_2$ $2H_2O$ (0.32 mg/mL), KCl (1.29 mg/mL) and NaCl (7.45 mg/mL) in water at pH 6 [37].

To 6 mL of freshly prepared mucin dispersions in SNF (1 mg/mL) held in a water bath (Julabo, Milan, Italy) at 37 °C under stirring (150 rpm), freeze dried SLN (or liposome) formulations, previously dispersed in 6 mL of SNF, were added. The turbidity of the stirred mixture at 37 °C was measured at

0, 2, 5, 7 and 24 h at the wavelength of 650 nm using a Perkin-Elmer Lambda Bio 20 spectrophotometer and compared with that of HEC dissolved in SNF at the concentration of 0.4 mg/mL taken as positive control. Each experiment was performed at room temperature in triplicate and the results are expressed as mean ± standard deviation of each mean.

2.7. X-Ray photoelectron spectroscopy (XPS) studies on SLN

XPS analysis of the SLN specimens, as well as the feed materials, was performed by a scanning microprobe PHI 5000 VersaProbe II (Physical Electronics, Chanhassen, MN), equipped with a monochromatized AlKα X-ray radiation source. The measurements were carried out in HP mode (scanned size about 1400 × 200 μm). Survey scans (binding energy (BE) range 0–1200 eV, FAT mode, pass energy 117.4 eV) and high-resolution spectra (FAT mode, pass energy 29.35 eV) were recorded for each sample. Quantification (atomic percentage, At%) and comparison of data from different elements were enabled by using peak areas normalized by empirically derived sensitivity factors, according to MultiPak library. Peak deconvolution has been done using the PHI-MultiPak software package (version 9.9.0). Charge referencing was performed by setting at 284.8 eV the lower binding energy C1s photo-peak (i.e., C1s hydrocarbon peak).

2.8. Cytotoxicity studies with Olfactory Ensheathing Cells (OECs)

OECs were isolated from mouse P2 olfactory bulbs as previously described [38,39]. OECs were plated on 25 cm^2 flasks and cultured in DMEM/FBS supplemented with a bovine pituitary extract. Cells were incubated at 37 °C in a fresh complete medium and were fed twice a week. Successively, OECs were plated at the number of 30,000 per each well of a 96-well plate. Cells were incubated with either plain SLN (0.25, 0.5, 1, 2.5, 5, and 10 μg/mL of lipids) in complete medium, or DA-SLN, or GCS-DA-SLN (same lipid concentrations corresponding to DA concentrations of 0.45, 0.9, 1.8, 4.5, 9.0. and 18 μM), or liposomal formulations Lip 1 and Lip 2 (0.25, 1, 4, 16, and 64 μg/mL of lipids, corresponding to DA concentrations of 0.3, 1.17, 4.7, 9, 18.75, and 75 μM). After 24 h, cells were tested for viability by the 3-(4,5-dimethylthiazol-2-yl)-2,5 diphenyl tetrazolium bromide (MTT) assay, as previously described [40]. The relative viability was calculated in respect to control untreated cells (considered as 100%). 1% Triton X-100-treated cells were used as positive control.

2.9. Uptake studies

OECs were plated at the number of 50,000 per each well of a 24-well plate. Cells were incubated with FITC-SLN (0.25-10 μg/mL of lipids) or 6-COUM-liposomal formulations (0.25-64 μg/mL) in complete medium. After 24 h, each well was treated with 0.04% trypan blue in PBS (in order to quench extracellular fluorescence), trypsinized, resuspended in 0.5 mL of PBS, and analysed by Amnis Flowsight IS100 (Merck). Brightfield scatter plots obtained by plotting Area on x-axis vs Aspect Ratio on y-axis were generated, then single cells events were gated, and finally 10,000 single-cell events for sample were acquired. The percentage of green positive cells (channel 2, 488 nm excitation laser) and mean fluorescence were analysed using Amnis IDEAS software [40].

2.10. Statistical analysis

Statistical analyses were carried out by Prism v. 4, GraphPad Software Inc., USA. Data were expressed as mean ± SD. Multiple comparisons were based on one-way analysis of variance (ANOVA) with the either Bonferroni's or Tukey's post hoc test and differences were considered significant when $p < 0.05$.

3. Results

In Table 1, the main physicochemical features of DA-loaded liposomes and SLN prepared by DRV and melt homogenization methods, respectively, are summarized. Among others, it can be deduced from Table 1 that DA-loaded CS-GSH coated liposomes (Lip 2) showed a mean diameter lower than the corresponding uncoated vesicles (Lip 1). Such significant size decrease has been accounted for the three different extrusion treatment through cut-off membrane filters used for the former vesicles preparation, unlike the latter ones [18]. Moreover, SLN 2 displayed a significant size reduction compared to the control ones (i.e., GCS-SLN) and this result was ascribed to a conformational reorganization of the GCS in the presence of the neurotransmitter, leading to GCS-DA-SLN shrinkage [33]. However, the most relevant finding was the higher E.E.% observed for SLN compared with the liposome formulations, particularly when SLN 2 is considered for which an E.E.% of 81% was observed. The PDI values of DA-loaded liposomes and SLN were in the range 0.16-0.27 suggesting, on the whole, a narrow size distribution while, in the case of SLN 2 and control SLN, the PDI values were higher implying a broader size distribution. Except for Lip 1 and control SLN, the zeta potentials of the investigated formulations were low in absolute value, whereas the introduction of the polycationic materials represented by CSGSH and GCS for liposomes and SLN, respectively, induced a positive surface charge (Table 1). Further physicochemical characterizations of liposomes and SLN nanocarriers herein studied, including physical and oxidative stability of vesicles as well as

the infrared spectroscopy in attenuated total reflectance mode (FT-IT/ATR) and thermogravimetric analyses (TGA) of SLN are reported in ([18] and [33]) to which the reader is referred to.

[Insert Table 1]

3.1. Stability studies on DA-loaded SLN

The low zeta potential in absolute values observed for DA-loaded liposomes and SLN suggested that an in-depth study on the physical stability of both formulations was mandatory. While such a study has already been reported for the vesicle formulations suggesting that Lip 2 is stable against oxidative damage up to 6 days of storage [18], herein, physical stability of SLN in the presence and in the absence of GCS was assessed at 4 °C, evaluating both particle mean diameter and neurotransmitter content evolution over the time. As reported in Fig. 1a, SLN 2 underwent to significant particle size decrease at the latest time points ($p<0.001$), whereas SLN 1 mean particle size was kept constant up to 1 month and, afterwards, particle size markedly increased ($p<0.001$) together with grey-black precipitate formation, indicative of particle aggregation and autoxidation of the active DA. Concerning DA content in SLN 2, it was essentially equal to the starting value within 2 weeks but, after 1 month of storage, half of the original DA amount was found ($p<0.001$) (Fig. 1b). The same trend in DA content was observed for SLN 1 even if the decrease in neurotransmitter amount at longer exposure times was lower than that observed for SLN 2. By comparing the SLN formulations with the vesicle Lip 1 and Lip 2 ones, it seems that the former preparations possess a greater physical stability. In particular, SLN 2 appear promising in terms of storage since their mean diameter and DA content can be maintained essentially constant for two weeks. Moreover, it should be pointed out that only after three months of storage at 4 °C, a change to pale grey colour of SLN 2 freeze-dried powders was noted by visual inspection, suggesting chemical (oxidative and hydrolytic) degradation is starting. Probably, the greater physical stability of SLN 2 formulation should be due to the amount of the neurotransmitter inside the nanocarrier. Furthermore, the localization of the neurotransmitter inside the nanocarrier and not on the surface, indeed, is expected to safeguard it from chemical degradation for a longer time [18].

[Insert Figure 1]

3.2. Mucoadhesive properties of DA-loaded liposomes and SLN

In view of the *in vivo* administration through the nasal mucosa, the *in vitro* mucoadhesive properties of DA containing liposomes and SLN were assessed by turbidimetric measurements carried out in SNF. Indeed, once DA-loaded liposomes- and SLN-mucin aggregates are formed by mixing each mixtures of these nanocarrier suspensions with mucin dispersion in the same medium, then an incubation time-dependent decrease in transmittance takes places [41]. For these experiments, powders of freeze-dried liposomes and SLN were directly dispersed in SNF and the changes in transmittance at 650 nm wavelength were recorded, comparing the results with those of HEC included as positive control. HEC, indeed, is endowed with good mucoadhesive characteristics, even though lower than Carbopol 974P [42] which, on the other hand, could not be employed due to its precipitation in SNF under conditions we used. Furthermore, after visual inspection, no change in colour of the tested formulations throughout the study was observed and it suggests that no chemical (oxidative and hydrolytic) degradation occurs. As shown in Fig. 2 among all tested formulations Lip 2 and SLN 1 showed mucoadhesive properties comparable with those of HEC. Interestingly, the highest decrease in transmittance after 24 h of incubation time was observed for SLN 2 followed by Lip 1 which both resulted in statistically significant difference compared with control ($p<0.001$ and <0.01 *vs* HEC, respectively).

Hence, based on the turbidimetric measurements after 24 h incubation time, the observed rank order of mucoadhesive properties for the examined formulations is the following: SLN 2 > Lip 1 > SLN 1, Lip 2 > HEC and, in particular, the most mucoadhesive formulation resulted SLN 2.

[Insert Figure 2]

3.3. XPS studies

XPS analysis of the SLN, with or without GCS and DA, was carried out in order to gain information on the surface chemical composition as well as on the possible modifications or interactions between the different components within the investigated formulations. The pure neurotransmitter and all the SLN components were analyzed as well. In Table 2, the atomic percentages of the elements detected on the sample's surfaces are reported. As for the XPS analyses of Lip 1 and Lip 2 formulations, they were previously reported and discussed [18]. In Fig. 3, the C1s curve fitting of the pure SLN components were reported.

As far as DA C1s signal is concerned (Fig. 3a), two components have been used to fit the signal: one at 284.8 eV, representing the C-C, C=C and C-H groups (plus contamination) and one at 286.3 eV, typical of C-OH and carbon linked to ammonium salts. The peak ratio was found to be 1.7:1, in total

agreement with that expected from the stoichiometry of dopamine molecule. For GCS (Fig. 3b), four contributions were detected on carbon signal. In particular, the first at 284.8 eV, was typical of hydrocarbons (plus contamination); the second, at 285.4, was typical of amine groups; the third at 286.4 eV, was relevant to C-OH and C-NH_3^+ groups and finally the fourth peak, falling at 287.9 eV, was ascribable to the carbohydrates O-C-O linkage. The two components of SLN formulations, i.e., Gelucire 50/13 and Tween 85 (Fig.s 3c and 3d), presented both a five-peak C1s curve fitting, with different relative abundances, in agreement with the molecular formulas of these organic compounds. Precisely, hydrocarbon peak at 284.8 eV, a peak in α-position to a carboxylic group at 285.4 eV, an alcoholic peak at 286.3 eV, a carbonyl group at 287.3 eV and a carboxylic one at 288.8 eV were detected. Moreover, C1s signals relevant to plain SLN and SLN 2 formulations were curve-fitted and shown in Fig.s 3e and f, respectively, evidencing no additional contributions to the curve-fitting with respect to those present in the feed materials, although in different relative abundances. Overall, based on the higher neurotrasmitter E.E.% and physical stability, the better mucoadhesion performance and the sustained release without burst effect [29,33]. SLN 2 was identified as the most interesting formulation for nose-to-brain DA delivery worthy of deeper *in vitro* and *ex vivo* studies.

[Insert Table 2 and Figure 3]

3.4. MTT studies on OECs

In order to see whether either the different SLN formulations were toxic in their way to the olfactory cells, OECs were incubated with plain SLN (not coated with GCS and not loaded with DA), SLN 1, or SLN 2 and cell viability was assessed after 24 h by the MTT assay. As shown in Fig. 4a, plain SLN were slightly toxic to OECs only at 5 and 10 μg/mL with a reduction of cell viability of around 20%. Interestingly, both SLN 1 and SLN 2 were not toxic to OECs at any concentration tested as compared with the appropriate control (untreated cells) (Fig. 4b and 4c).

[Insert Figure 4]

Liposomal formulations were tested by the same assay and at the same time point. It is worth to consider that lipid concentrations are different from those present in SLN 1 and SLN 2 in order to

obtain similar DA concentrations. However, Lip1 and Lip2 were not toxic to OEC cells, at tested lipid concentrations (Fig. 5).

[Insert Figure 5]

3.5. Uptake studies by OECs

Given the highest mucoadhesion properties presented by SLN 2, FITC-SLN 2 were prepared for uptake studies. Cell uptake was studied in OECs following incubation for 24 h. Fig. 6a shows that the FITC-SLN 2 were internalised by an increasing percentage of cells, reaching the 100% at 5 μg/mL. This behaviour was paralleled by the increase in the mean fluorescence intensity (Fig. 6b). Overall, these results indicate that the internalisation of SLN by OECs is mediated by a dose-response process.

[Insert Figure 6]

Uptake studies were also performed with liposomal formulations. Uncoated liposomes (Lip 1) were internalised in a dose-dependent manner obtaining only 9.0 ± 3.9% of positive cells at 16 μg/mL and, to further test the cell uptake capability of these liposomes, 27 ± 12.5% of positive cells with four-times higher concentration (64 μg/mL) (Fig. 7a), while the mean fluorescence intensity peaked already at 4 μg/mL (Fig. 7b). Interestingly, the coated formulation (Lip 2) was internalized by around 71% of cells with the highest lipid concentration (Fig. 7c), and with 1 μg/mL and above the mean fluorescence intensity was consistently higher as compared to the lowest concentration (Fig. 7d). Of note, the highest concentration (64 μg/mL) was not toxic to OECs (Fig. 5).

[Insert Figure 7]

4. Discussion

In the present work, DA-loaded-liposomes and -SLN were investigated in a comparative manner with the aim to evaluate their potential for nose-to-brain neurotransmitter delivery. For this purpose, in the first step of the study, attention was paid to the preparative aspects consisting in maximizing the

encapsulation efficiency of the neurotransmitter in each of these nanocarrier types. While it is well known that hydrophilic substances as DA can be encapsulated in liposome aqueous core, in the case of SLN the encapsulation of water-soluble drugs, such as therapeutic peptides/proteins, is characterized by a low loading efficiency, mainly due to the leakage of the drug during nanoparticle preparation [43]. Thus, encapsulation of hydrophilic compounds in SLN is not a simple task and, indeed, it constitutes a challenge for scientists involved in the field. On the other hand, even liposome formulations may undergo drug leakage due to change of phospholipid bilayer integrity consequent to oxidation and chemical hydrolysis of phospholipids occurring in aqueous medium [26, 44]. It seems that an appropriate polymer coating (e.g. chitosan, alginate) may limit such drug leakage from vesicle formulations [45]. The most employed approach for an acceptable preparation of hydrophilic drug-loaded SLN is the double emulsification (W/O/W) method endowed with, however, both a toxicological concern related to the use of organic solvents and tendency of globules to coalesce, leading to an increase of nanoparticle size [30]. In this regard, we are involved in demonstrating that the use of a self-emulsifying lipid in the melt homogenization method for SLN preparation, could be a simple and alternative approach to double emulsification (W/O/W) method for preparing hydrophilic drug-loaded SLN with satisfactory loading efficiency [30]. It follows from the hypothesis that, being a nano-emulsion formed once the self-emulsifying lipid is in the presence of water, the hydrophilic compound may be entrapped in the nano-emulsion, but the following fast lipid recrystallization during the cooling process may limit the diffusion of the hydrophilic compound towards the aqueous external phase and the consequent leakage. We have shown the feasibility of this approach in the encapsulation of the antioxidant tripeptide glutathione and the grape seed extract proanthocyanidins for which E.E.% up to 82.7 % was found for the former [33] and a loading efficiency of 5.8% (comparable with that observed in the encapsulation of proanthocyanidins in a hydrophilic matrix as chitosan) was observed for the latter [40].

In the case herein examined of the neurotransmitter DA encapsulation in liposomes and SLN, data in Table 1 clearly show that vesicle formulations lead to unsatisfactory encapsulation efficiency even using DA-loaded CS-GSH coated liposomes (Lip 2) (*i.e.,* 12.2 ± 0.3%) and, hence, a polymer coating of vesicles provided only a limited benefit. On the other hand, the E.E.% of SLN 1 was higher than that of Lip 2 resulting of 19 ± 3% which markedly increased to 81 ± 2 % when SLN 2 were examined. Hence, this positive result obtained with the hydrophilic neurotransmitter DA further supports the suggestion that SLN based on self-emulsifying lipid as Gelucire® 50/13 may be used to encapsulate hydrophilic compounds with satisfactory loading efficiency. Moreover, in this preparative approach, the association of the polycation GCS to DA-loaded Gelucire® 50/13 SLN seems most advantageous and it should be considered for a further increase the E.E.% of hydrophilic substances. This finding

is also interesting if compared with the recent result reported in a manuscript [46] where DA-loaded SLN made of glycerol tripalmitin/octadecylamine are described with an encapsulation efficiency at most of 70% and a lower storage stability (*i.e.,* 30% loss of DA content over one week of storage at 4 °C in the better case; [46].

Concerning the findings of the mucoadhesion study on lipid formulations herein evaluated, the best mucoadhesive performance was observed for SLN 2. This result may be explained on the basis of the zeta potential recorded for these nanocarriers which, even though slightly positive, should allow electrostatic interactions with negatively charged mucus proteins leading to efficient adhesion [31]. Such zeta potential value of SLN 2 should be related to the association of polycation GCS whose good mucoadhesive performance are known [31, 47,48]. Hence, among the examined formulations, in the nasal cavity SLN 2 should better interact with mucus and increase residence time facilitating absorption [15]. The significant mucin interaction of negatively charged uncoated DA-loaded vesicles Lip 1 greater than the corresponding coated ones with CSGSH (Lip 2) is somewhat surprising if we consider that the high mucoadhesive properties of thiomers as CSGSH [31]. However, it should be also taken into account that, on the basis of XPS study previously carried out on these liposomes, it was evidenced that the -SH groups of the thiomer CS-GSH are not exposed outside the vesicles since no sulfur was detected on the surface [18]. Therefore, the thiol-disulfide exchange reactions with mucus protein chains responsible of improved mucoadhesive properties of thiomers should be reduced or absent at all, explaining so the lower mucoadhesion of Lip 2 compared with Lip 1 [18, 31].

The most interesting results deduced from XPS studies are summarized in Table 2. As shown, on GCS-SLN control, no nitrogen was detected, suggesting that GCS was not present on the surface. On the other hand, the N1s atomic percentages in SLN 1 and SLN 2 were quite similar, even if their E.E.% were significantly different, as already reported [33]. However, since XPS studies only the surface composition of the samples, the similar nitrogen percentage is an indirect evidence of the drug massive presence in the internal layers, especially SLN 2, as highlighted by E.E.% data.

As far as DA C1s signal is concerned (Fig. 3a), the C-H_x/C-OH peak ratio was found to be 1.7:1, in total agreement with that expected from the stoichiometry of dopamine molecule. In GCS (Fig. 3b), the C-NH_2/O-C-O peak ratio was 0.96:1, indicating an almost totally neutral state of the bare macromolecule. In Gelucire 50/13 (Fig. 3c), the COH/COOR corrected area ratio was found to be 7:1, while in Tween 85 (Fig. 3d), the same ratio was 12:1. In the case of plain SLN (Fig. 3d), it is evident that the surface chemistry is in between the one of the two components (*i.e.*, Gelucire 50/13 and Tween 85), in agreement with that already reported [21]. Indeed, the COH/COOR was found to be 10:1. On the other hand, the presence of GCS in SLN 2 did not change the C1s curve fitting (Fig.

3f), as also verified in C1s signal relevant to GCS-SLN surface (Fig. 1S). Indeed, no O-C-O contribution, typical of GSC, was detected, indicating no allocation of GCS on the nanoparticle surface, irrespectively from the DA presence in the formulation. On the other hand, a huge C-OH peak increase (with a COH/COOR ratio equal to 24:1) was recorded on SLN 2 surface. This could be probably ascribable to a surface enrichment in Tween, but the presence of dopamine, with C-OH and C-NH_3^+ groups falling both at 286.3 eV, cannot be excluded. Actually, the DA presence on surface was also confirmed by the detection of the N1s signal. As far as SLN 1 is concerned, the C1s curve fitting resulted quite similar to that of SLN 2 (Fig. 2S). In addition, the nitrogen atomic percentages in SLN 1 and SLN 2 resulted comparable (Table 2), even if the encapsulation efficiency percentage (E.E. %) and the *in vitro* release of DA from these systems, already reported [33], resulted significantly different. All these findings let us to argue that in the SLN 2 nanocarriers, differently from the SLN 1, the neurotransmitter was not located on surface except for a negligible amount but encapsulated in the internal layers of the nanoparticles, leading to a very promising DA reservoir system. Moreover, the slightly positive zeta potential recorded for SLN 2, indicative of a surface GCS presence, was apparently in contrast with XPS evidences but it cannot be ruled out that in the wet physical state, where zeta potential measurements are performed, it can happen a partial rising of the GCS chains to the surface. This finding was not observed by XPS since in this technique particles were not examined in liquid suspension but at solid dry state [49].

The findings of these studies could be interpreted in the context of the model proposed by us for PEGylated SLN as the Gelucire® 50/13-based SLN [29]. Indeed, following a literature hint about PEG2000−stearic acid based SLN structure [50], we suggested that Gelucire® 50/13-based SLN are constituted by a hydrophilic shell of polyoxyethylene chains of solid lipid (Gelucire® 50/13) and cosurfactant (Tween 85) together with an internal lipid core comprising the stearoyl moieties (Fig. 8a) [29]. This implies that a hydrophilic substance as the neurotransmitter DA, could be adsorbed on the particle surface or entrapped in the hydrophilic shell as well as encapsulated in the lipid core as nano-emulsion and this is the case of SLN 1 formulation *i.e.,* the so called outer-shell distribution [[51]]. However, in such circumstances, immature leakage of the neurotransmitter adsorbed on the particle surface or entrapped in the hydrophilic shell could occur during sample manipulations lowering the corresponding E.E.%. When these PEGylated SLN were associated to GCS, this polycation should be localized inside the nanoparticles since on GCS-SLN control no nitrogen was detected by XPS analysis (Table 2). More precisely, the polycation should be localized within the hydrophilic shell because only in this layer formation of a network compact structure could occur arising from hydrogen bonding and polar interactions between the polyoxyethylene chains of Gelucire® 50/13 and GCS (Fig. 8b). In the case of SLN 2 formulation, besides in the lipid core as

nano-emulsion, the neurotransmitter DA should be localized in the hydrophilic shell due to hydrogen bonding and polar interactions involving the polyoxyethylene chains, GCS and the functional groups of DA. In this last case, however, the presence of the mentioned network could hamper the leakage of DA entrapped in the hydrophilic shell accounting for the marked increase in E.E.% observed for SLN 2 compared with SLN 1. In short, formation of the mentioned network structure in SLN 2, but not in SLN 1, accounts for the marked increase in E.E.% since the leakage of the neurotransmitter entrapped in internal layers in the former formulation should be hampered. Moreover, formation of the mentioned network structure could also explain the greater physical stability of SLN 2 compared with SLN 1 since it allows the localization of the neurotransmitter inside, but not on the surface of the nanocarrier for a longer time. However, it should be taken into account that, as far as the structures of the particles is concerned in SLN, further aspects remain to be clarified, including the arrangements of the lipids and stabilizing agents during the particles formation [52]. Overall, the model proposed for the Gelucire® 50/13-based PEGylated SLN could be also useful to interpret the results of *in vitro* release studies [18, 34].

[Insert Figure 8]

It is worth noting that plain SLN were quite toxic at high concentrations of lipid, whereas those SLN containing DA (both SLN 1 and SLN 2) were not. DA has been shown to reduce ferroptosis in cancer and non-cancer cells and increase cell viability at 12-5-50 μM by reducing glutathione depletion and malondialdehyde production [52]. Of note, some studies have reported a cytoprotective effect of L-DOPA, e.g. by inducing the synthesis of GSH in cultured cells [52,53], suggesting a role of DA against oxidative stress, although we have not ruled out these events in our experimental conditions. It has been also found that DA increased proliferation of subventricular zone-derived cells inducing the release of EGF [54], an effect that could take part in its cytoprotective role in OECs. Concerning uptake studies, in the literature, fluorescent polymersomes of PEG-PLGA have been already loaded with 6-COUM to investigate brain delivery in mice and, therefore, we selected the same probe 6-COUM in order to have affinity for the lipophilic vesicles, being 6-COUM a hydrophobic dye [55]. Interestingly, liposomal formulations seem to be less efficient than SLN in the uptake process, and the uncoated ones the lesser than the uncoated, although the mean fluorescence intensity reached similar levels considering all the SLN and liposomal nanoparticles. With four-times higher concentration, the coated liposomal formulation Lip 2 reached around 70% of positive cells. Overall,

these results indicate that, in face of a similar average entry of fluorescent formulations, it is the number of cells that varies so that SLN can deliver DA in all the cells which they come into contact with at lipid concentrations lower than liposomes. Moreover, it is also suggested that delivering DA via the olfactory route with SLN would be more efficient than using liposomes.

The lack of cytotoxicity of DA-containing SLN experienced in our results is in good achievement of a safe transport of these compounds through the olfactory region of nasal cavity. First of all, the property of mucoadhesion would limit the mucociliary clearance of the drug in the vestibular region of the nose. In the posterior region of nasal cavity, the transport of the DA-containing nanoparticles would occur following different routes to the brain, among which of interest is the interaction with the endings of olfactory receptor neurons, from which it will be transported following the nerve channel created by OECs through the cribriform plate and finally entering into the cerebrospinal fluid and olfactory bulb [56]. SLN 2, endowed with the highest mucoadhesion properties, were also taken up with high efficiency by OECs (reaching the 100% of positive cells), making possible to consider DA transport to the brain via OECs a safe way.

5. Conclusions

DA-loaded SLN 1 and SLN 2 have been investigated, in comparison with DA-loaded vesicles Lip 1 and Lip 2, to test their feasibility for non-invasive nose-to-brain delivery approach applied to PD treatment. The high E.E.% observed for SLN 2 (81%), their better physical stability in terms of storage (*i.e.,* mean diameter and DA content essentially constant for two weeks) combined with their good mucoadhesion properties and lack of cytotoxicity towards OECs make these PEGylated nanocarriers as interesting candidates for further studies ruling out the alternative lipid formulations (*i.e.,* SLN 1 and Lip 1 and Lip 2). Although to the best of our knowledge no formulation for nasal administration is still available for PD treatment, this work envisages new perspectives of the potential of this route of administration for a neurological disorder such as PD.

Acknowledgements

This work was partially financed by University of Bari (Italy) to A.T. (Cod. CUP:H91J11000160001). A.T. would also acknowledge Dr. Tatiana Brenna (Gattefossè, Italy) for providing Gelucire® 50/13 lipid and Dr. Francesca Curci and Dr. Licia Anna Pugliese for their valuable technical assistance.

Declaration of interests: The authors declare that they have no known competing financial interests or personal relationships that could have appeared to influence the work reported in this paper.

[1] L. Hirsch, N. Jette, A. Frolkis, T. Steeves, T. Pringsheim, The Incidence of Parkinson's Disease: A Systematic Review and Meta-Analysis, Neuroepidemiology, 46 (2016) 292-300.
[2] E. Wollmer, S. Klein, A review of patient-specific gastrointestinal parameters as a platform for developing in vitro models for predicting the in vivo performance of oral dosage forms in patients with Parkinson's disease, Int J Pharm, 533 (2017) 298-314.
[3] A. Di Stefano, P. Sozio, A. Iannitelli, L.S. Cerasa, New drug delivery strategies for improved Parkinson's disease therapy, Expert Opin Drug Deliv, 6 (2009) 389-404.
[4] S. Di Gioia, A. Trapani, D. Mandracchia, E. De Giglio, S. Cometa, V. Mangini, F. Arnesano, G. Belgiovine, S. Castellani, L. Pace, M.A. Lavecchia, G. Trapani, M. Conese, G. Puglisi, T. Cassano, Intranasal delivery of dopamine to the striatum using glycol chitosan/sulfobutylether-beta-cyclodextrin based nanoparticles, Eur J Pharm Biopharm, 94 (2015) 180-193.
[5] C. Rodriguez-Nogales, E. Garbayo, M.M. Carmona-Abellan, M.R. Luquin, M.J. Blanco-Prieto, Brain aging and Parkinson's disease: New therapeutic approaches using drug delivery systems, Maturitas, 84 (2016) 25-31.
[6] F. Re, M. Gregori, M. Masserini, Nanotechnology for neurodegenerative disorders, Maturitas, 73 (2012) 45-51.
[7] M. Conese, R. Cassano, E. Gavini, G. Trapani, G. Rassu, E. Sanna, S. Di Gioia, A. Trapani, Harnessing Stem Cells and Neurotrophic Factors with Novel Technologies in the Treatment of Parkinson's Disease, Curr Stem Cell Res Ther, 14 (2019) 549-569.
[8] C. Saraiva, C. Praca, R. Ferreira, T. Santos, L. Ferreira, L. Bernardino, Nanoparticle-mediated brain drug delivery: Overcoming blood-brain barrier to treat neurodegenerative diseases, J Control Release, 235 (2016) 34-47.
[9] G.H. Hawthorne, M.P. Bernuci, M. Bortolanza, V. Tumas, A.C. Issy, E. Del-Bel, Nanomedicine to Overcome Current Parkinson's Treatment Liabilities: A Systematic Review, Neurotox Res, 30 (2016) 715-729.
[10] S. Pillay, V. Pillay, Y.E. Choonara, D. Naidoo, R.A. Khan, L.C. du Toit, V.M. Ndesendo, G. Modi, M.P. Danckwerts, S.E. Iyuke, Design, biometric simulation and optimization of a nano-enabled scaffold device for enhanced delivery of dopamine to the brain, Int J Pharm, 382 (2009) 277-290.
[11] E. De Giglio, A. Trapani, D. Cafagna, L. Sabbatini, S. Cometa, Dopamine-loaded chitosan nanoparticles: formulation and analytical characterization, Anal Bioanal Chem, 400 (2011) 1997-2002.
[12] A. Trapani, E. De Giglio, D. Cafagna, N. Denora, G. Agrimi, T. Cassano, S. Gaetani, V. Cuomo, G. Trapani, Characterization and evaluation of chitosan nanoparticles for dopamine brain delivery, Int J Pharm, 419 (2011) 296-307.
[13] R. Pahuja, K. Seth, A. Shukla, R.K. Shukla, P. Bhatnagar, L.K. Chauhan, P.N. Saxena, J. Arun, B.P. Chaudhari, D.K. Patel, S.P. Singh, R. Shukla, V.K. Khanna, P. Kumar, R.K. Chaturvedi, K.C. Gupta, Trans-blood brain barrier delivery of dopamine-loaded nanoparticles reverses functional deficits in parkinsonian rats, ACS Nano, 9 (2015) 4850-4871.
[14] E.R. Rashed, H.A. Abd El-Rehim, M.A. El-Ghazaly, Potential efficacy of dopamine loaded-PVP/PAA nanogel in experimental models of Parkinsonism: possible disease modifying activity, J Biomed Mater Res A, 103 (2015) 1713-1720.
[15] V. Bourganis, O. Kammona, A. Alexopoulos, C. Kiparissides, Recent advances in carrier mediated nose-to-brain delivery of pharmaceutics, Eur J Pharm Biopharm, 128 (2018) 337-362.
[16] E. Samaridou, M.J. Alonso, Nose-to-brain peptide delivery - The potential of nanotechnology, Bioorg Med Chem, 26 (2018) 2888-2905.
[17] A. Trapani, D. Tricarico, A. Mele, F. Maqoud, D. Mandracchia, P. Vitale, V. Capriati, G. Trapani, V. Dimiccoli, A. Tolomeo, A. Scilimati, A novel injectable formulation of 6-fluoro-l-DOPA imaging agent for diagnosis of neuroendocrine tumors and Parkinson's disease, Int J Pharm, 519 (2017) 304-313.
[18] A. Trapani, D. Mandracchia, G. Tripodo, S. Cometa, S. Cellamare, E. De Giglio, P. Klepetsanis, S.G. Antimisiaris, Protection of dopamine towards autoxidation reaction by encapsulation into non-coated- or chitosan- or thiolated chitosan-coated-liposomes, Colloids Surf B Biointerfaces, 170 (2018) 11-19.
[19] H. Li, P. Yang, W. Knight, Y. Guo, J.S. Perlmutter, T.L.S. Benzinger, J.C. Morris, J. Xu, The interactions of dopamine and oxidative damage in the striatum of patients with neurodegenerative diseases, J Neurochem, 152 (2020) 235-251.

[20] A. Ancona, M. Sportelli, A. Trapani, R.A. Picca, C. Palazzo, E. Bonerba, F. Mezzapesa, G. Tantillo, G. Trapani, N. Cioffi, Synthesis and Characterization of Hybrid Copper-Chitosan Nano-antimicrobials by Femtosecond Laser-Ablation in Liquids, Material Letters, 136 (2014) 397-400.
[21] D. Mandracchia, A. Rosato, A. Trapani, T. Chlapanidas, I.M. Montagner, S. Perteghella, C. Di Franco, M.L. Torre, G. Trapani, G. Tripodo, Design, synthesis and evaluation of biotin decorated inulin-based polymeric micelles as long-circulating nanocarriers for targeted drug delivery, Nanomedicine, 13 (2017) 1245-1254.
[22] A. Singh, H.L. Kutscher, J.C. Bulmahn, S.D. Mahajan, G.S. He, P.N. Prasad, Laser ablation for pharmaceutical nanoformulations: Multi-drug nanoencapsulation and theranostics for HIV, Nanomedicine, 25 (2020) 102172.
[23] M. Agrawal, S. Saraf, S.G. Antimisiaris, N. Hamano, S.D. Li, M. Chougule, S.A. Shoyele, U. Gupta, Ajazuddin, A. Alexander, Recent advancements in the field of nanotechnology for the delivery of anti-Alzheimer drug in the brain region, Expert Opin Drug Deliv, 15 (2018) 589-617.
[24] A. Trapani, V. Laquintana, A. Lopedota, M. Franco, A. Latrofa, G. Talani, E. Sanna, G. Trapani, G. Liso, Evaluation of new propofol aqueous solutions for intravenous anesthesia, Int J Pharm, 278 (2004) 91-98.
[25] G. Tripodo, G. Pasut, A. Trapani, A. Mero, F.M. Lasorsa, T. Chlapanidas, G. Trapani, D. Mandracchia, Inulin-D-alpha-tocopherol succinate (INVITE) nanomicelles as a platform for effective intravenous administration of curcumin, Biomacromolecules, 16 (2015) 550-557.
[26] T. Karamanidou, M. Agrawal, F. Saraf, F. Saraf, S.G. Antimisiaris, N. Hamano, S.-D. Li, M. Chougule, S.A. Shoyele, U. Gupta, Ajazuddin, A. Alexander, Recent advancements in the field of nanotechnology for the delivery of anti-Alzheimer drug in the brain region, Expert Opin Drug Deliv, 15 (2018) 589-617.
[27] G. Kaur, M. Arora, M.N.V. Ravi Kumar, Oral Drug Delivery Technologies-A Decade of Developments, J Pharmacol Exp Ther, 370 (2019) 529-543.
[28] G. Trapani, M. Franco, A. Trapani, A. Lopedota, A. Latrofa, E. Gallucci, S. Micelli, G. Liso, Frog intestinal sac: a new in vitro method for the assessment of intestinal permeability, J Pharm Sci, 93 (2004) 2909-2919.
[29] A. Trapani, G. Tripodo, D. Mandracchia, N. Cioffi, N. Ditaranto, V. De Leo, H. Cordero, M.A. Estebane, Glutathione-loaded solid lipid nanoparticles based on Gelucire® 50/13: Spectroscopic characterization and interactions with fish cells, J Drug Deliv Sci Tech, 47 (2018) 359-366.
[30] A. Trapani, D. Mandracchia, G. Tripodo, S. Di Gioia, S. Castellani, N. Cioffi, N. Ditaranto, M.A. Esteban, M. Conese, Solid lipid nanoparticles made of self-emulsifying lipids for efficient encapsulation of hydrophilic substances, in: AIP Conference Proceedings, 2019, pp. 020004.
[31] A. Trapani, C. Palazzo, M. Contino, M.G. Perrone, N. Cioffi, N. Ditaranto, N.A. Colabufo, M. Conese, G. Trapani, G. Puglisi, Mucoadhesive properties and interaction with P-glycoprotein (P-gp) of thiolated-chitosans and -glycol chitosans and corresponding parent polymers: a comparative study, Biomacromolecules, 15 (2014) 882-893.
[32] S.G. Antimisiaris, Preparation of DRV Liposomes, Methods Mol Biol, 1522 (2017) 23-47.
[33] S. Cometa, M.A. Bonifacio, G. Trapani, S. Di Gioia, L. Dazzi, E. De Giglio, A. Trapani, In vitro investigations on dopamine loaded Solid Lipid Nanoparticles, J Pharm Biomed Anal, 185 (2020) 113257.
[34] A. Trapani, D. Mandracchia, C. Di Franco, H. Cordero, P. Morcillo, R. Comparelli, A. Cuesta, M.A. Esteban, In vitro characterization of 6-Coumarin loaded solid lipid nanoparticles and their uptake by immunocompetent fish cells, Colloids Surf B Biointerfaces, 127 (2015) 79-88.
[35] S. Perteghella, D. Mandracchia, M.L. Torre, R. Tamma, D. Ribatti, A. Trapani, G. Tripodo, Anti-angiogenic activity of N,O-carboxymethyl-chitosan surface modified solid lipid nanoparticles for oral delivery of curcumin, J. Drug Deliv. Sci. Technol., 56 (2020) 101494.
[36] D. Mandracchia, A. Trapani, S. Perteghella, M. Sorrenti, L. Catenacci, M.L. Torre, G. Trapani, G. Tripodo, pH-sensitive inulin-based nanomicelles for intestinal site-specific and controlled release of celecoxib, Carbohydr Polym, 181 (2018) 570-578.
[37] S.A. Pagar, D.M. Shinkar, R.B. Saudagar, Development and evaluation of in situ nasal mucoadhesive gel of metoprolol succinate by using 3^2 full factorial design, Int. J. Pharm. Pharm. Sci., 6 (2014) 218-223.
[38] R. Pellitteri, M. Spatuzza, A. Russo, S. Stanzani, Olfactory ensheathing cells exert a trophic effect on the hypothalamic neurons in vitro, Neurosci Lett, 417 (2007) 24-29.
[39] T. Musumeci, R. Pellitteri, M. Spatuzza, G. Puglisi, Nose-to-brain delivery: evaluation of polymeric nanoparticles on olfactory ensheathing cells uptake, J Pharm Sci, 103 (2014) 628-635.

[40] S. Castellani, A. Trapani, A. Spagnoletta, L. di Toma, T. Magrone, S. Di Gioia, D. Mandracchia, G. Trapani, E. Jirillo, M. Conese, Nanoparticle delivery of grape seed-derived proanthocyanidins to airway epithelial cells dampens oxidative stress and inflammation, J Transl Med, 16 (2018) 140.
[41] S. Rossi, F. Ferrari, M.C. Bonferoni, C. Caramella, Characterization of chitosan hydrochloride-mucin interaction by means of viscosimetric and turbidimetric measurements, Eur J Pharm Sci, 10 (2000) 251-257.
[42] D. Ivarsson, M. Wahlgren, Comparison of in vitro methods of measuring mucoadhesion: ellipsometry, tensile strength and rheological measurements, Colloids Surf B Biointerfaces, 92 (2012) 353-359.
[43] L. Becker Peres, P.H.H. de Araujo, C. Sayer, Solid lipid nanoparticles for encapsulation of hydrophilic drugs by an organic solvent free double emulsion technique, Colloids Surf B Biointerfaces, 140 (2016) 317-323.
[44] N. Matougui, L. Boge, A.C. Groo, A. Umerska, L. Ringstad, H. Bysell, P. Saulnier, Lipid-based nanoformulations for peptide delivery, Int J Pharm, 502 (2016) 80-97.
[45] M.C. Woodle, Surface-modified liposomes: assessment and characterization for increased stability and prolonged blood circulation, Chem Phys Lipids, 64 (1993) 249-262.
[46] E. Ortega, S. Blanco, A. Ruiz, M.A. Peinado, S. Peralta, M.E. Morale, Lipid nanoparticles for the transport of drugs like dopamine through the blood-brain barrier, preprint in the Beilstein Archives, (2020).
[47] C. Palazzo, G. Trapani, G. Ponchel, A. Trapani, C. Vauthier, Mucoadhesive properties of low molecular weight chitosan- or glycol chitosan- and corresponding thiomer-coated poly(isobutylcyanoacrylate) core-shell nanoparticles, Eur J Pharm Biopharm, 117 (2017) 315-323.
[48] M.I. Adamczak, E. Hagesaether, G. Smistad, M. Hiorth, An in vitro study of mucoadhesion and biocompatibility of polymer coated liposomes on HT29-MTX mucus-producing cells, Int J Pharm, 498 (2016) 225-233.
[49] E.B. Souto, J.F. Fangueiro, R.H. Müller, Solid Lipid Nanoparticles (SLN™), in: I.F. Uchegbu, A.G. Schätzlein, W.P. Cheng, A. Lalatsa (Eds.) Fundamentals of Pharmaceutical Nanoscience, Springer, New York, NY, 2013, pp. 91-116.
[50] H. Yuan, C.Y. Chen, G.H. Chai, Y.Z. Du, F.Q. Hu, Improved transport and absorption through gastrointestinal tract by PEGylated solid lipid nanoparticles, Mol Pharm, 10 (2013) 1865-1873.
[51] A. Gordillo-Galeano, C.E. Mora-Huertas, Solid lipid nanoparticles and nanostructured lipid carriers: A review emphasizing on particle structure and drug release, Eur J Pharm Biopharm, 133 (2018) 285-308.
[52] D. Wang, Y. Peng, Y. Xie, B. Zhou, X. Sun, R. Kang, D. Tang, Antiferroptotic activity of non-oxidative dopamine, Biochem Biophys Res Commun, 480 (2016) 602-607.
[53] M.A. Mena, V. Davila, D. Sulzer, Neurotrophic effects of L-DOPA in postnatal midbrain dopamine neuron/cortical astrocyte cocultures, J Neurochem, 69 (1997) 1398-1408.
[54] G.C. O'Keeffe, P. Tyers, D. Aarsland, J.W. Dalley, R.A. Barker, M.A. Caldwell, Dopamine-induced proliferation of adult neural precursor cells in the mammalian subventricular zone is mediated through EGF, Proc Natl Acad Sci U S A, 106 (2009) 8754-8759.
[55] Y. Yu, Z. Pang, W. Lu, Q. Yin, H. Gao, X. Jiang, Self-assembled polymersomes conjugated with lactoferrin as novel drug carrier for brain delivery, Pharm Res. 29 (2012) 83-96.

[56] M. Agrawal, S. Saraf, S. Saraf, S.G. Antimisiaris, M.B. Chougule, S.A. Shoyele, A. Alexander, Nose-to-brain drug delivery: An update on clinical challenges and progress towards approval of anti-Alzheimer drugs, J Control Release, 281 (2018) 139-177.

Captions to Figures

Fig. 1. a) Particle size changes over the time of SLN incubated for 8 weeks at 4°C; b) DA content changes over the time after storage of SLN at 4 °C for 8 weeks. Each experiment was performed in triplicate and the results are expressed as mean ± standard deviation of each mean. Blue bars refer to incubation of SLN 1 and red bars refer to SLN 2. For all sample sets, the value referring to time zero was taken as control. ** $p < 0.001$ *vs* control. (For interpretation of the references to colour in this Fig. legend, the reader is referred to the web version of this article).

Fig. 2. Mucoadhesive properties in SNF of a) Lip 1 (green), Lip 2 (black), SLN 1 (blue) and SLN 2 (red). HEC (magenta) was taken as positive control. (For interpretation of the references to colour in this Fig. legend, the reader is referred to the web version of this article).

Fig. 3. C1s curve fittings of DA (a), GCS (b), Gelucire 50/13 (c) and Tween 85 (d) and formulations (plain SLN (e) and SLN 2 (f)). Uncertainty on BE peak positions was ±0.2 eV.

Fig. 4. Cytotoxicity of SLN derivatives. OECs were challenged with plain-SLN (a) for 24 h at the indicated concentrations (μg/mL). SLN 1 (b) and SLN 2 (c) were used at the same lipid concentrations, resulting in DA as 0.45, 0.9, 1.8, 4.5, 9.0 and 18 μM. Cells were then assayed for vitality by the MTT assay. Controls (CTRL) are untreated cells (100% of vitality), whereas 1% Triton X-100 (TX) was used as positive control. **$p<0.05$; ***$p < 0.0001$ *vs* CTRL. Data are the results of two-three experiments each carried out in four wells.

Fig. 5. Cytotoxicity of liposomal formulations. OECs were challenged with Lip1 (a) and Lip2 (b) for 24 h at the indicated concentrations (μg/mL), obtaining DA concentrations of 0.3, 1.17, 4.7, 9.0 and 18.75, and 75 μM. Cells were then assayed for vitality by the MTT assay. Controls (CTRL) are untreated cells (100% of vitality), whereas 1% Triton X-100 (TX) was used as positive control. ***$p < 0.0001$ *vs* CTRL. Data are the results of two experiments each carried out in four wells.

Fig. 6. Cellular uptake of FITC-SLN 2 by OECs. OECs were incubated with the indicated concentrations (μg/mL) of FITC-SLN 2 for 24 h and evaluated by flow cytometry. Positive cells, shown as percentages (a), and the mean fluorescence intensity (b), were obtained in three experiments each conducted in triplicate. In a) **$p<0.001$ and ***$p<0.0001$ (in black) denote differences between 0.25 *vs* 1.0, 2.5, 5.0 and 10.0; *$p<0.05$, **$p<0.001$ and ***$p<0.0001$ (in gray) denote differences between 1.0 *vs* 2.5, 5.0 and 10.0. In b) **$p<0.001$ denotes differences between 0.25 and 10; *$p<0.05$ denotes differences between 1.0 and 2.5 *vs* 10.0.

Fig. 7. Cellular uptake of FITC-liposomal formulations by OECs. OECs were incubated with the indicated concentrations (μg/mL) of Lip1 (a, b) or Lip 2 (c, d) for 24 h and evaluated by flow cytometry. Positive cells, shown as percentages (A, C), and the mean fluorescence intensity (b, d), were obtained in two experiments each conducted in triplicate. In A) *$p<0.05$ denote differences between 0.25 and 1 *vs* 64. In b) *$p<0.05$ denotes differences between 0.25 *vs* 16. In c), **$p<0.001$ denotes differences between 0.25 *vs* 4 and 16, while ***$p<0.0001$ between 0.25 *vs* 64. In d), *$p<0.05$ denote differences between 0.25 *vs* 4.

Fig. 8. Schematic representation of the a) PEGylated SLN 1; b) PEGylated SLN 2.

Fig. 1S. C1s signal relevant to GCS-SLN

Fig. 2S. C1s signal relevant to DA-GCS-SLN

Figure

Click here to access/download;Figure;Figure 1 JPEG.jpg

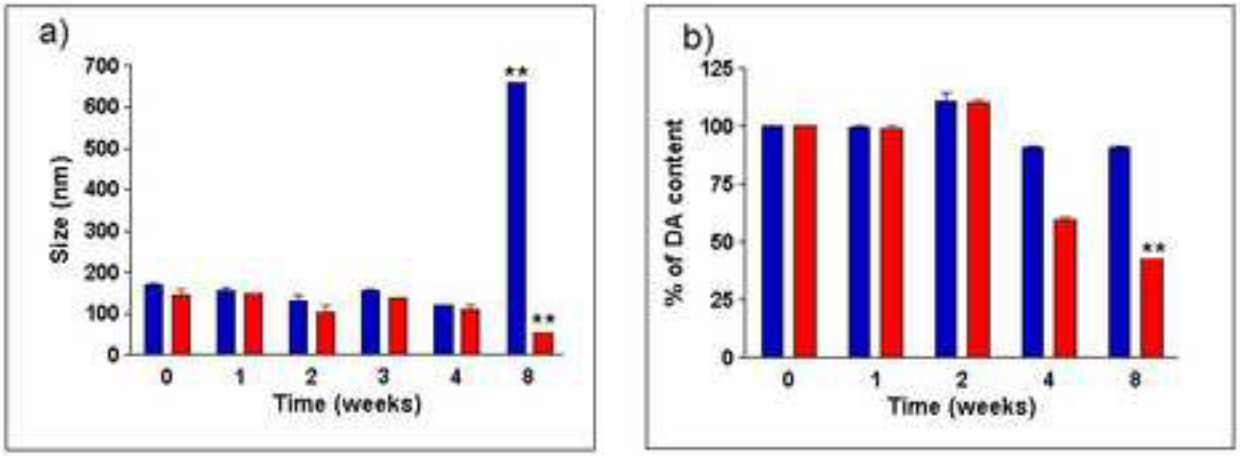

Figure

Click here to access/download;Figure;Figure 2 JPEG.jpg

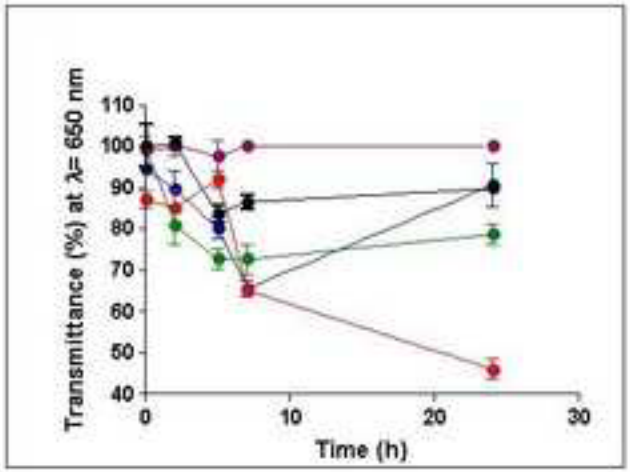

Figure

Click here to access/download;Figure;Figure 3 JPEG.jpg

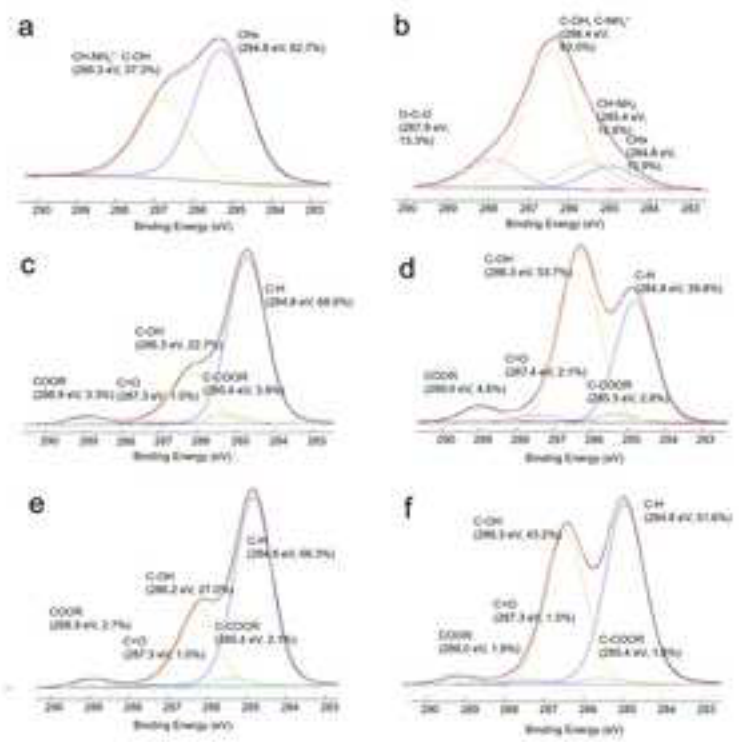

Figure

Click here to access/download;Figure;Figure 4 JPEG.jpg

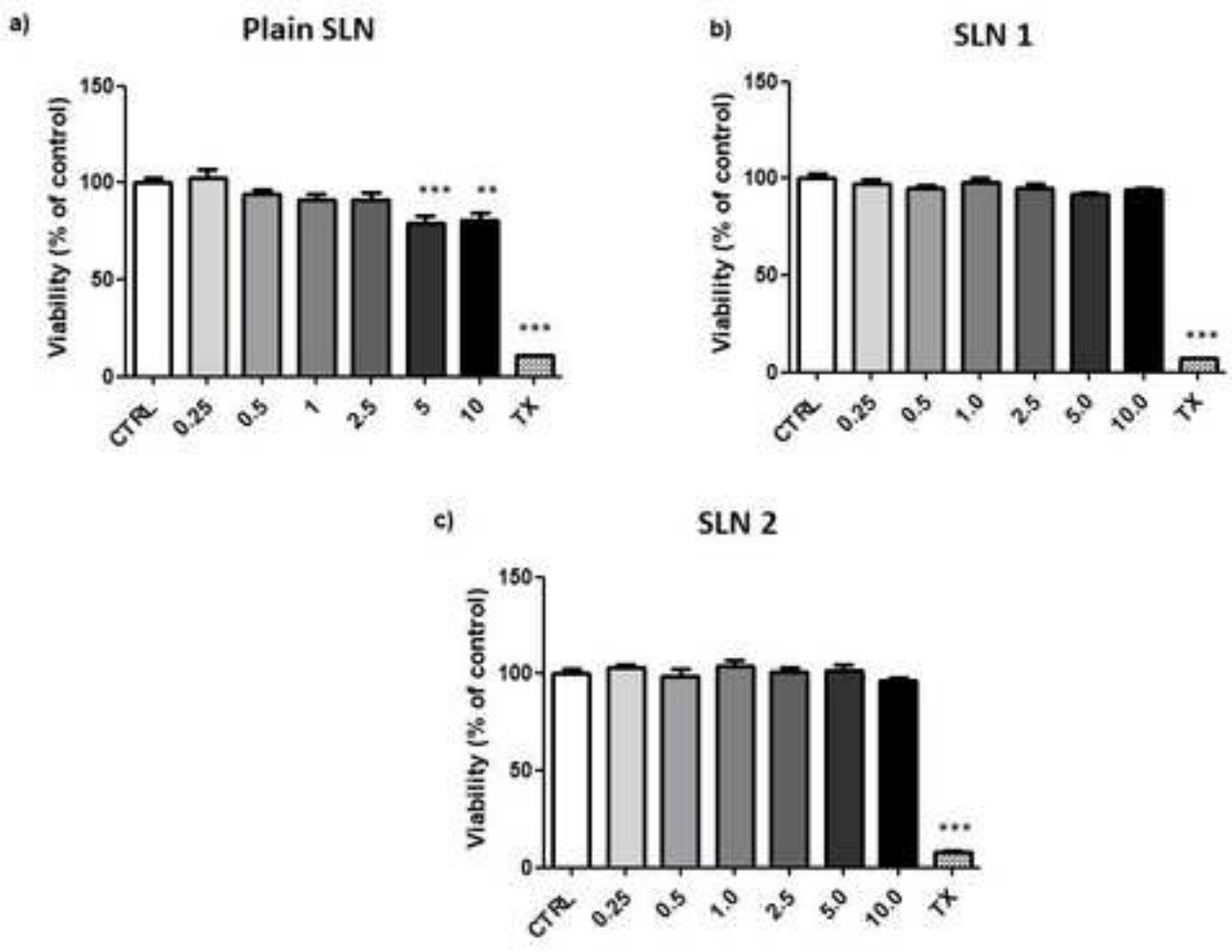

Figure

Click here to access/download;Figure;Figure 5 JPEG.jpg

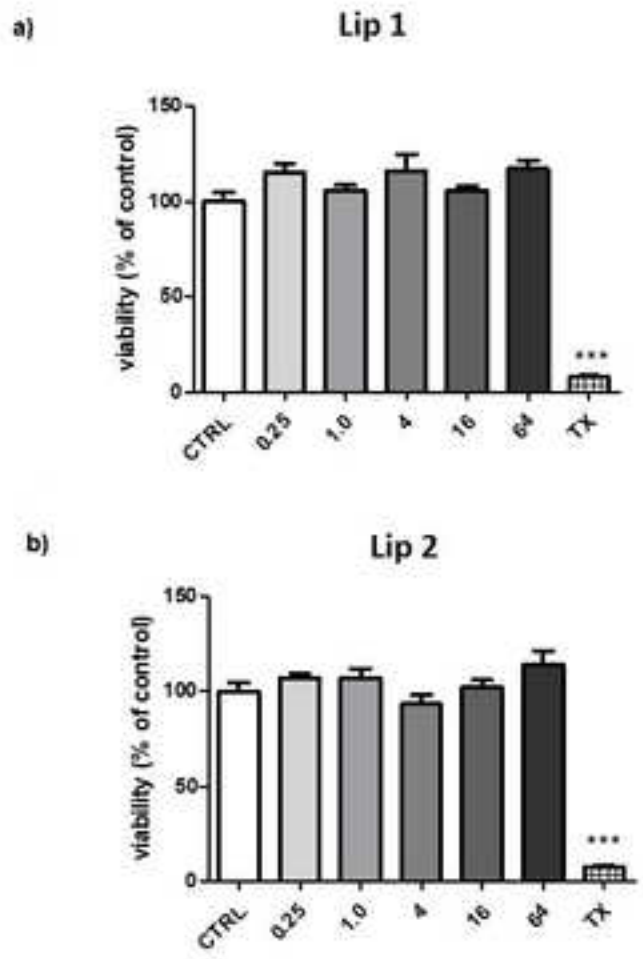

Figure

Click here to access/download;Figure;Figure 6 JPEG.jpg

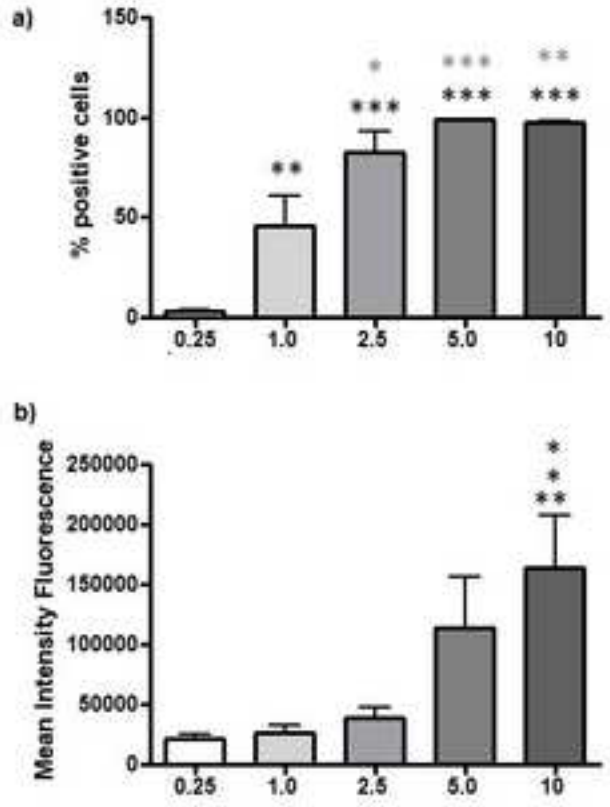

Figure

Click here to access/download;Figure;Figure 7 JPEG.jpg

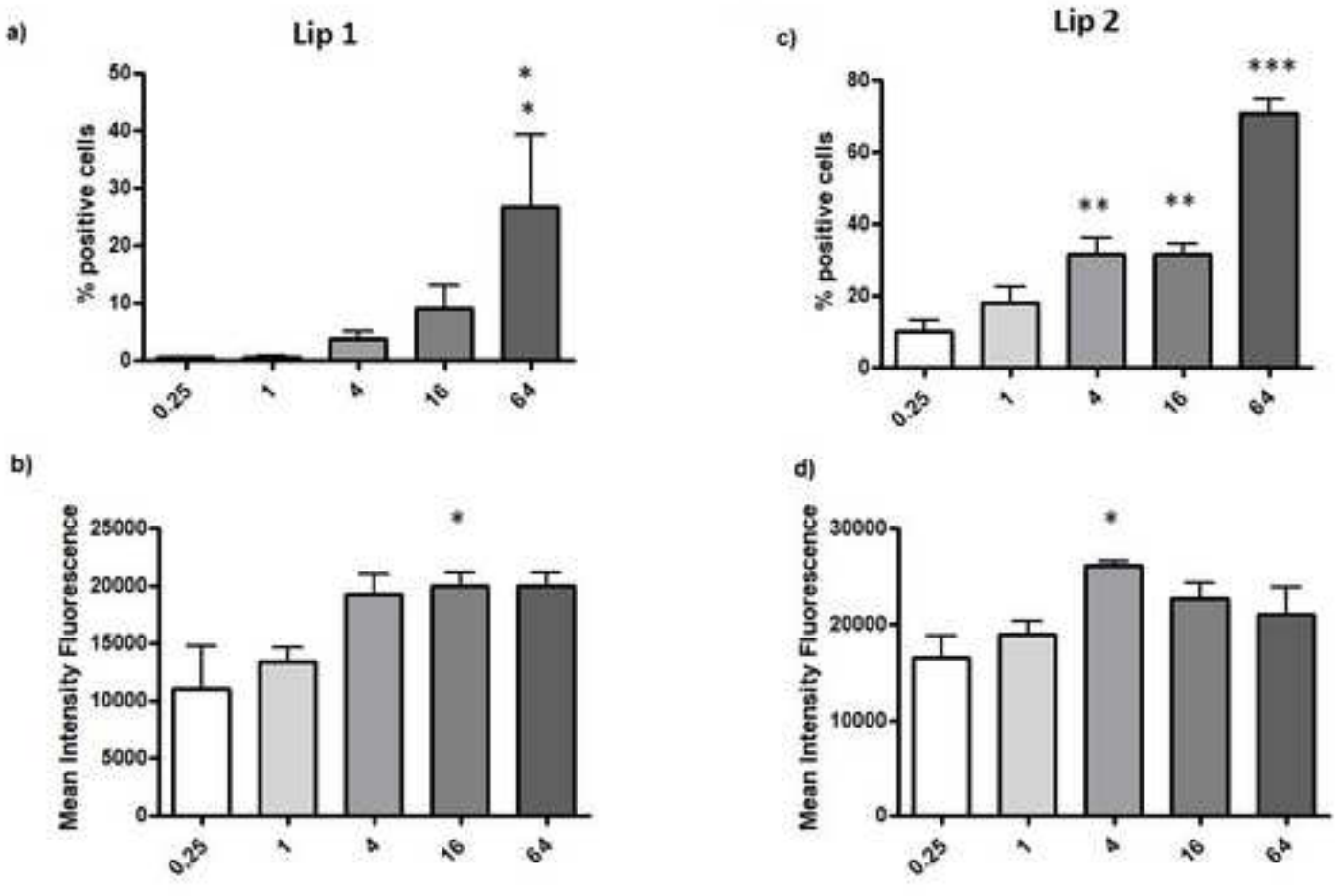

Figure

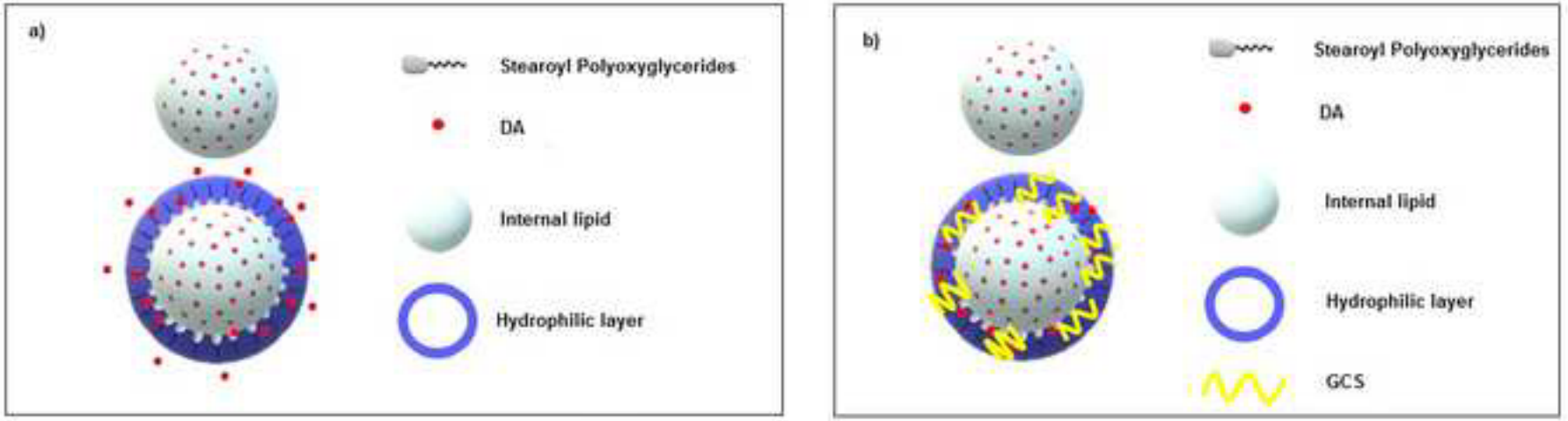

Figure

Click here to access/download;Figure;Figure 1S JPEG.jpg

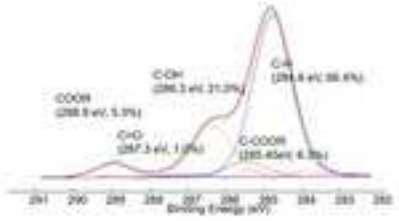

Figure

Click here to access/download;Figure;Figure 2S JPEG.jpg

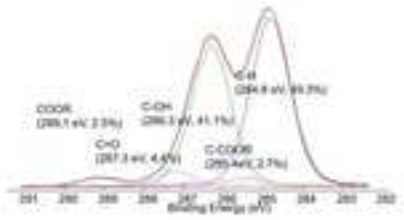

Table

Table